UCLA
Adaptive Optics for Extremely Large Telescopes 4 – Conference Proceedings

Title
INO Pyramidal Wavefront Sensor Demonstrator: first closed-loop on-sky operation at Mont-Mégantic Telescope

Permalink
https://escholarship.org/uc/item/1k41x51n

Journal
Adaptive Optics for Extremely Large Telescopes 4 – Conference Proceedings, 1(1)

Authors
Martin, Olivier
Turbide, Simon
Legace, Francois
et al.

Publication Date
2015

DOI
10.20353/K3T4CP1131575

Copyright Information
Copyright 2015 by the author(s). All rights reserved unless otherwise indicated. Contact the author(s) for any necessary permissions. Learn more at https://escholarship.org/terms

Peer reviewed

eScholarship.org Powered by the California Digital Library
University of California

INO Pyramidal Wavefront Sensor Demonstrator: first closed-loop on-sky operation at Mont-Mégantic Telescope

Olivier Martin*[a], Simon Turbide[a], François Lagacé[a], Frédéric Lévesque[a], Philippe Goyette[a], Geneviève Anctil[a], François Châteauneuf[a], Denis Brousseau[b], William Deschênes[b,d] ,Jean-Pierre Véran[c],

[a]Institut National d'Optique, 2740 rue Einstein, Québec, QC, G1P 4S4 Canada; [b] Université Laval**,** 2325 rue de l'Université, Québec, QC G1V 0A6**,** Canada; [c]Herzberg Institute of Astrophysics, NRC-CNRC, 5071 West Saanich Road, Victoria, BC V9E 2E7, Canada; [d]ABB measurement systems, 585 bd Charest Est, Suite 300, Quebec, QC CA G1K 9H4

ABSTRACT

Wavefront sensing is one of the key elements of an Adaptive Optics System. As an alternative to the commonly encountered, commercially available Shack-Hartmann WFS (SH-WFS), the more recent Pyramid-WFS (P-WFS) is proving to be a very attractive technology, thanks to its high-sensitivity and robustness against aliasing. At INO, center for applied research in optics and technology transfer in Quebec City, Canada, we have developed a compact and flexible P-WFS prototype that can be integrated into an AO system. This P-WFS prototype includes a fast piezo-electric modulation mirror and a high-sensitivity EMCCD camera. Our P-WFS was installed on the experimental AO system developed by Laval University in Quebec for the 1.6-m Mont-Mégantic telescope, which also includes a commercial high-speed SH-WFS. The architecture is such that both WFSs can take measurements simultaneously, and either one can be used to drive the deformable mirror. Here we present the on-sky results obtained with the INO P-WFS module.

Keywords: Adaptive optics, Wavefront sensor, Pyramid, PWFS, Demonstrator, INO

1. INTRODUCTION

The present work takes place in the framework of an internal development project that started at INO in 2010. At the time the goal was to gain experience with adaptive optics systems and especially with the concept of Pyramid wavefront sensors. INO specializes in technology developments in optics and photonics and one of its missions is to assist companies from Canada and abroad during development phases at intermediate technology readiness levels. As no other Canadian institute had any experience with P-WFS, the topic presented a good opportunity. P-WFS were not as readily available commercially as the Shack-Hartmann wavefront sensors, yet seemed to offer high potential with possible applications in astronomy but also in bio-medical imaging, ophthalmology, microscopy, etc. A laboratory demonstrator was built, based upon a monolithic pyramid prism, with low-cost active components and single wavelength source. Results presented at the AO4ELT3 conference[1] were promising, with good agreement between simulation and experiment in terms of wavefront reconstruction error. Subsequently a series of upgrades was implemented to INO`s P-WFS prototype with the intention to carry out field tests on a telescope[2] and eventually to compare the performance of Pyramid and Shack-Hartmann (SH) sensors in the same conditions. The Mont-Mégantic Telescope AO facility was developed by Laval University and is presented in another poster at this conference[3]. First on-sky tests happened in June 2015. Although a number of system limitations in conjunction with poor weather conditions prevented us from taking data that would have allowed a direct comparison of P-WFS and SH, some valuable data were obtained with the AO loop closed. In the following paragraph the P-WFS principle of operation is briefly recalled. Paragraph 3 shows the experimental set-up and the on-sky test results are presented in chapter 4.

*olivier.martin@ino.com; phone 1 418 657-7006 ext. 2720; fax 1 418 657-7009; www.ino.com

2. PRINCIPLE OF OPERATION

The Pyramid wavefront sensor (P-WFS) is an evolution of the standard Foucault knife-edge test to allow a quantitative estimation of the spatial derivative of the wavefront distortion. It was first proposed by Ragazzoni[4] in 1996 and since then successfully implemented on large telescopes AO systems like the one at LBT[5].

The principle of operation is shown in Figure 1. Four images of the entrance pupil – itself conjugate to the telescope pupil – are produced by a pyramid-shaped prism onto the detector by means of a telecentric lens system. Modulation of the pupil by means of a tip-tilt mirror is necessary to extend the linearity range of the sensor and telecentricity of the system ensures that pixels remain co-registered in the four pupil images in the detector plane as the pupil is modulated.

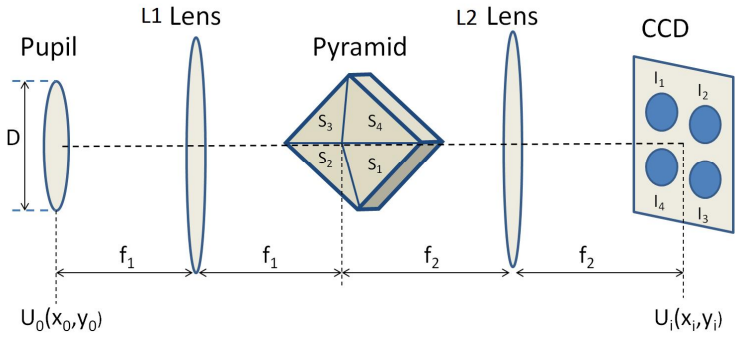

Figure 1. Schematic representation of the P-WFS.

The P-WFS signals are defined as a combination of the four pupil images averaged over the modulation period:

$$S_x(x,y) = \langle I_1(x,y)\rangle + \langle I_4(x,y)\rangle - \langle I_2(x,y)\rangle - \langle I_3(x,y)\rangle$$
$$S_y(x,y) = \langle I_1(x,y)\rangle + \langle I_2(x,y)\rangle - \langle I_3(x,y)\rangle - \langle I_4(x,y)\rangle \quad (1)$$

where the coordinates (x,y) refer to co-registered pixels in the four pupil images, as defined in Figure 2. In the limit of small aberrations the P-WFS signals can be decomposed in a sum of interaction matrices, themselves functions of Zernike polynomials. Wavefront reconstruction is then derived from the response matrix combined from the measured *x* and *y* signals.

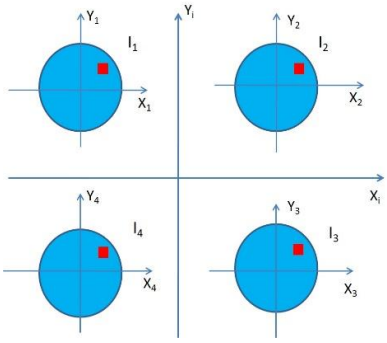

Figure 2: Definition of the four pupil images in the detector plane. The red squares indicate co-registered pixels.

3. P-WFS MODULE FOR ON-SKY TESTS

INO's P-WFS demonstrator was originally built out of laboratory components, not suitable to be taken out for real life experiments. This section gives a summary of the upgrade work done in 2015 to convert the prototype into a robust modular system, improve its sensitivity with faint sources and increase its acquisition speed. The first goal was to take

part to on-sky test campaigns at the focus of Mont-Mégantic Observatory 1.6m telescope. To do so the P-WFS module would need to be interfaced to the AO on-sky test bench designed and built by Laval University.

3.1 Optical design

3.1.1 Sensor stage

As seen in Figure 1 the Pyramid wavefront sensor is made of five elements: a modulation device (tip-tilt mirror) placed at a pupil at the entrance of the system, a long focal length lens L1 that focuses the beam at the apex of the pyramid, a pyramid prism, a short focal length lens L2 that projects the four sub-pupils on the camera. Modulation mirror and camera are active components that limit the speed and sensitivity of the P-WFS.

The original L1 lens between the TTM and pyramid was re-used due to its good optical quality over an extended spectral range and because the very large f/ number (f/45) provided a large depth of field.

The pyramid prism is also the same monolithic prism from the original demonstrator. Its apex is slightly rectangular, 50µm by 30µm, which is smaller than the 85µm spot diameter. The pyramid asymmetry results in sub-pupil intensity imbalance; I_1 and I_3 are brighter than I_2 and I_4 for a non-aberrated input wavefront.

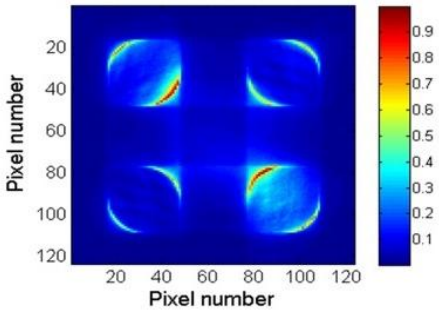

Figure 3: Pupil images produced by a slightly asymmetric pyramid (actual data from the original P-WFS demonstrator)

The magnification lens between pyramid and camera was upgraded to an achromatic doublet optimized for the 650-1050nm range. Its focal length was chosen in order to minimize the effects of chromatic dispersion of the sub-pupils on the camera. When the camera is binned 4x4 the spread between images at 600nm and 800nm is less than $1/10^{th}$ of a metapixel which in principle allows the WFS to work over the extended spectral range compared to the original demonstrator single-wavelength. If the case of images left unbinned then the chromatic spread represents $1/3^{rd}$ of a pixel over a 41 pixel wide sub-pupil.

The modulation mirror is a fast piezo tip-tilt actuator from Physik Instrumente. The model S-330K415 is a modified S-330.4Sx (1-inch mirror, 2-axis) with 4kHz resonant frequency and ±2.3mrad closed loop excursion. In principle the maximum operating frequency is about $1/3^{rd}$ of the resonance frequency but the actual limit is set by the amplifier. With the mirror weight the capacitive load is 6µF and the Bode plot for the E-505 series amplifier used here has a 3dB roll-off of about 500Hz. This frequency corresponds to closed-loop operation on a full travel of the mirror. The P-WFS actually needs about $1/5^{th}$ of the full travel to produce 5 λ/D modulations.

The camera was upgraded to a back-illuminated Electron Multiplying CCD from Nüvü Cameras, model HNü 512, thermoelectrically cooled to -90°C. Pixels size is 16 µm. Maximum frame rate (unbinned) is about 200 fps. To achieve ~500 fps it is necessary to use 4x4 binning and Regions of Interest on the camera. Such a binning factor would also provide almost perfect one-to-one matching between DM actuators and sub-pupil pixels. The set-up developed by Laval University for Mt-Mégantic telescope uses a 97-actuator ALPAO DM to close the AO loop; in the widest dimensions there are 11x11 actuators. If the telescope pupil is sampled on the 10x10 DM actuators footprint then there can be one to one relationship between the telescope sub-pupils and P-WFS sub-pupils metapixels with the camera used in 4x4 binning.

3.1.2 Calibration stage

In the laboratory the P-WFS is aligned and calibrated on a test bench that includes a fiber-pigtailed Thorlabs SLS201 white light source, a visible light phase-only Holo-eye SLM for the generation of controlled aberrations and two optical relays to adjust the beam diameter. Pellicle beam splitters placed in the collimated beam provide one extra arm where a

DM will be positioned conjugate both to the SLM plane and P-WFS modulation mirror pupil plane and one arm for control of the beam quality with a commercial wavefront sensor. The DM had not been implemented yet in this phase of the project. The overall layout is shown in Figure 4.

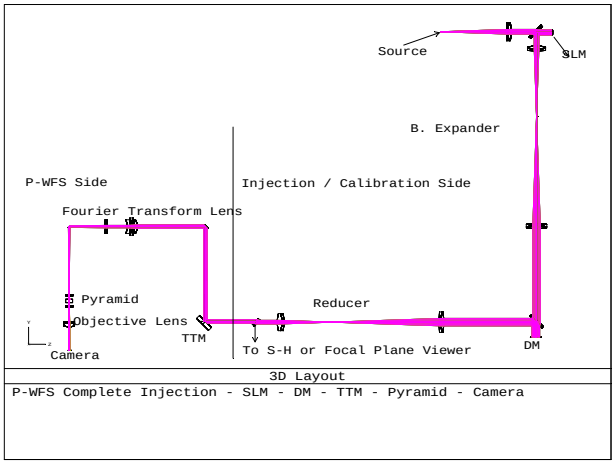

Figure 4. Optical layout of the pyramid wavefront sensor test-bench for laboratory characterization.

3.2 Mechanical design

A significant effort was provided on the design of the P-WFS module mechanical structure. Finite Element Analysis (FEA) was done on the CAD design to ensure that minimal flexures occur when the system is attached to the mechanical interface on the Mont-Mégantic telescope AO test bench built by Laval University in Québec. The weight of the camera (about 5kg) placed at a large lever arm was taken into account. Movements of the telescope down to 30° zenith angle are allowed. The P-WFS module total weight is about 12kg. Figure 5 shows the P-WFS module during initial alignment.

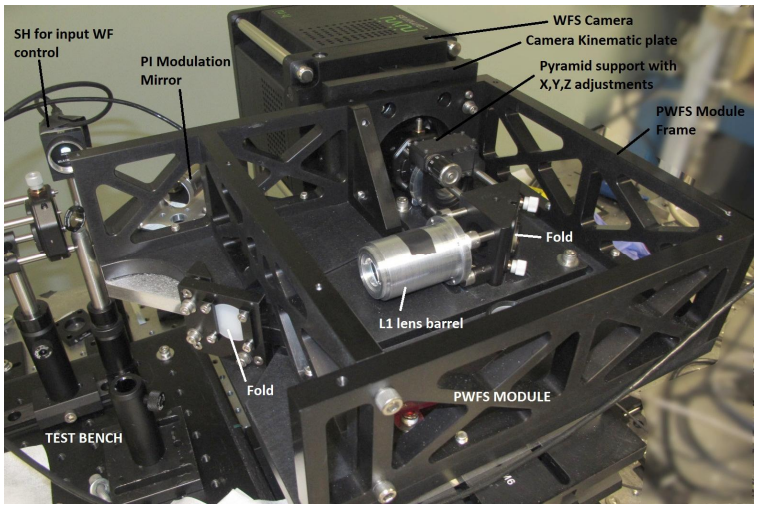

Figure 5. P-WFS module on the laboratory test bench at INO.

The module is pre-aligned at INO and only a set of fold mirrors need to be adjusted afterwards at integration on the telescope. The camera kinematic allows excellent repeatability of positioning so that no alignment is necessary when the camera is removed then re-installed. Figure 6 shows the P-WFS attached to the AO test bench during integration at Laval University.

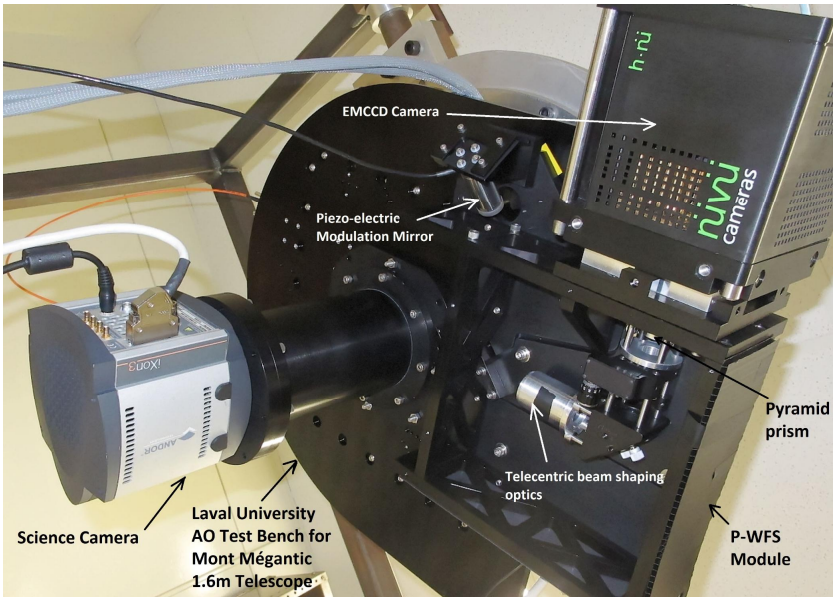

Figure 6: P-WFS module attached to the AO Test bench at Laval University before integration on the telescope.

4. INTEGRATION ON THE TELESCOPE AO TEST BENCH

Due to delays with the integration of active components the preparation and debug work of the system occurred in the short period of time before the actual on-sky run at Mont-Mégantic Observatory. The overall system performance was hampered by a number of limitations that appeared:

- External trigger of the camera acquisition by the piezo modulation mirror proved more difficult than expected due to some jitter and dead time between the command and start of frame. The camera has to integrate over exactly one turn of the modulation mirror. This was only possible by measuring the dead time which depended on the frame rate. Eventually some delay parameters were hard-coded in the camera and mirror control software so that only a set of acquisition frequencies were available. The fastest frame rate that could be achieved (regardless of binning, 1x1 or 4x4) was 175Hz. Upgrade of the camera internal software has been recently provided by the manufacturer and will solve these problems for future work.
- Vignetting of the beam on the AO test bench upstream of the P-WFS made the exact definition of a pupil mask difficult. One-to-one matching of P-WFS metapixels and DM actuators was not accurate enough in 4x4 binning so eventually P-WFS frames were kept unbinned for the calculations of command matrices. Also only modal calibration of the P-WFS to DM response proved efficient. When zonal calibration was attempted the peripheral dead zones of the DM (vignetted or outside the beam footprint) prevented from closing the AO loop in a stable way. Although 1x1 binning was not optimal because of possible blurring of the sub-pupils due to the chromatic dispersion over the 200nm spectral band pass, this chromatic effect was probably less noticeable than all other problems encountered. No major difference was seen between P-WFS images taken through a 100nm or 200nm band-pass filter. Figure 7 shows a P-WFS frame during integration tests when the loop was closed on the AO test bench Shack-Hartmann and a calibration source. Residual aberrations from the alignment errors of optics are visible both on the SH and P-WFS; vignetting mainly affects the P-WFS. Figure 8 shows the system installed on the 1.6m telescope during afternoon checks before a night of observing.
- Lack of time prevented from optimizing the interface software between the P-WFS and DM control. Whereas the SH control was straightforward and already implemented with the object-oriented Alpao Core Engine software, the calculation of interaction matrices and command matrices in the case of P-WFS required slow Matlab commands, external files saves and input/output that limited the overall process speed. As a result the loop was closed on sky at only 7 to 12 Hz on the P-WFS.
- No IR camera was available on time for the June 2015 run. Instead a silicon based EMCCD was used so the actual wavelength band for AO image correction on sky was 700 to 900nm (Z' band). AO correction would

have been more efficient in H band, as the telescope mirror sampling is 1.6m/10 = 16cm and under average seeing at Mont Mégantic Observatory the value of r0 is less than 10cm in Z' Band.

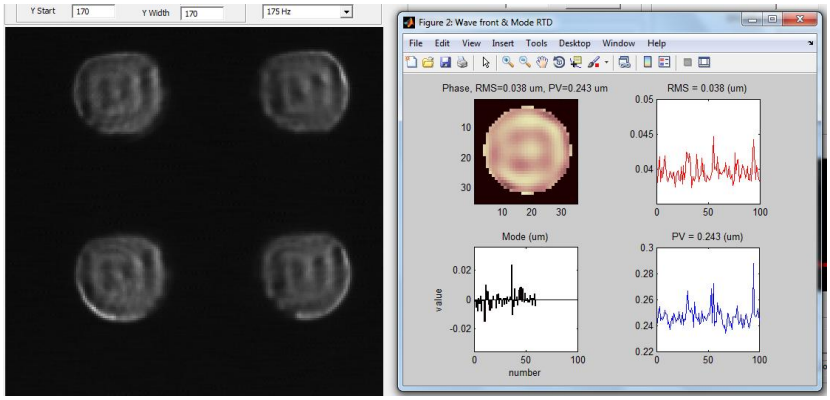

Figure 7: image of the P-WFS subpupils (left) and residuals as measured on the AO test bench Shack-Hartmann (right)

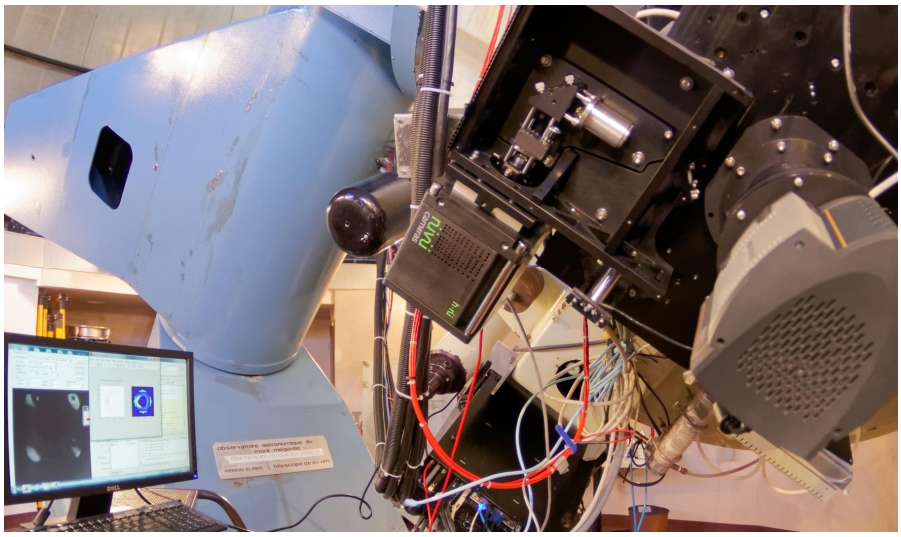

Figure 8: pre-observing calibration tests. On the screen: effect on P-WFS sub-pupils of one DM actuator poked at a time (plus ≈1λ defocus on the DM).

5. ON-SKY RESULTS

Bad weather during the observing run reduced the actual time on sky to less than three nights, during which the seeing conditions were mediocre, at best 2 arcsec and sky transparency was reduced. Furthermore the light throughput in the AO test bench when attached to the telescope Cassegrain focus was reduced and attempts to close the loop were only successful on two bright stars, Arcturus and Vega in the case of P-WFS. By comparison the loop was closed on the SH only on Arcturus as there was insufficient light flux with Vega. No actual comparison between SH and P-WFS were possible because of these adverse conditions; nevertheless some data was taken and are summarized below. The AO loop was stable on the PWFS only with the first 12 Zernike terms corrected, which contributes to the reduced efficiency of image correction.

The P-WFS output signal (Sx and Sy) defined in Eq. (1) are shown in 9 in open-loop and closed-loop on-sky operations and 1x1 binning on the EMCCD. As expected, the P-WFS signals are more flat on close-loop operation, which indicate that some wavefront error has been compensated by the deformable mirror. In this example, it appears that the dominant

wavefront errors are tip/tilt. The ~ 15 pixels diameter circle at the center of each Sx and Sy image corresponds to the central obstruction of the telescope.

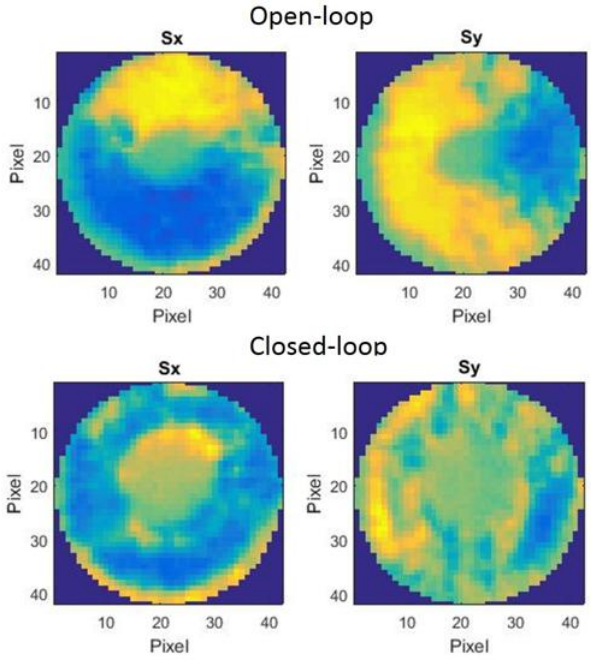

Figure 9: P-WFS output signal (Sx and Sy) for open-loop (top) and closed-loop (bottom) on-sky operations.

For each cycle of commands on sky the PWFS Influence Matrix on the DM is calculated as follows: knowing the matrix of measured slopes $S_{measured}$, and by calibration during pre-observing tests the matrix of slopes responses to specific Zernike modes H, then $S_{measured}$ = H*c where c is the proportion of Zernike modes. As the command vector is cmdVector=K*c, where K is the matrix of given currents for specific modes, then we have:

cmdVector=K*pinv(H)* $S_{measured}$ (2),

and the PWFS Influence Matrix is IM=K*pinv(H),

where pinv(H) is the pseudo-inverse matrix of H calculated in Matlab (Moore-Penrose pseudo-inverse).

The time evolution of the P-WFS signal variances are shown in 10 for closed-loop and open-loop on-sky operation. The variance for open-loop is about three times larger than for closed-loop operation, indicating the AO system compensates for some wavefront aberration induced by the atmospheric turbulence. Finally, Figure 11 show the Arcturus (top) and Vega (bottom) images collected by the Science camera. Over long exposures the FWHM for Arcturus images is reduced from an elliptical 56x82 pixels (open loop) to 36x32 pixels (closed loop) and for Vega images the FWM goes from 43x56 pixels (open loop) to 39x30 pixels (closed loop), signaling that some degree of correction is achieved.

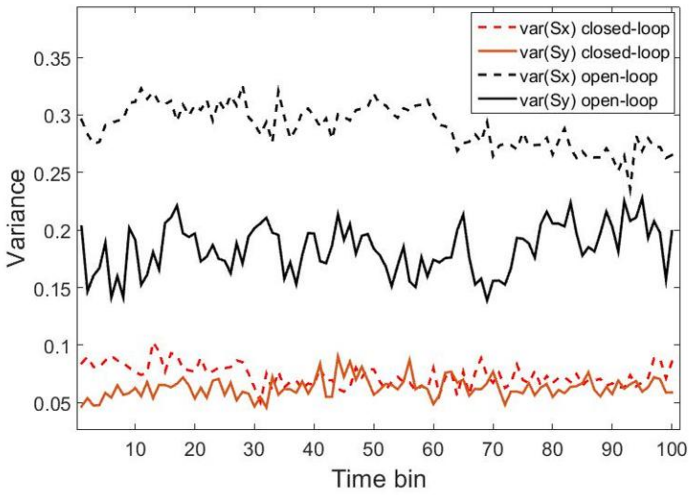

Figure 10: Variance of the Sx and Sy signal as a function of time, for closed-loop and open-loop operations.

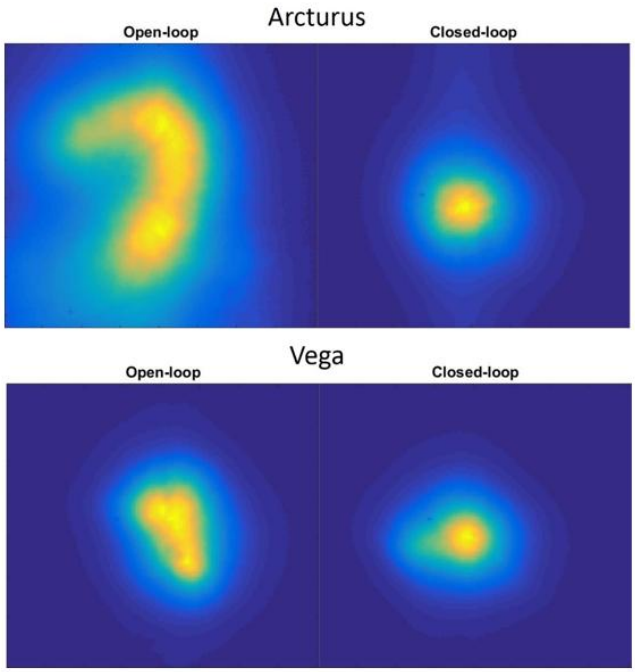

Figure 11: Arcturus (top) and Vega (bottom) images with and without AO operation. 12 Zernike polynomials corrected with loop closed on P-WFS.

6. CONCLUSION

Upgrades on the Pyramid Wavefront Sensor demonstrator at INO have made the module available for integration on the AO on-sky test bench developed for the Mont-Mégantic Observatory Telescope. A first observing run occurred in June 2015. Although the original intent to compare near-simultaneous on-sky performance of Shack-Hartmann and Pyramid wavefront sensors was not possible given the limited amount of time for the preparation of the test campaign, we managed to close the loop on individual star images. The AO loop was stable and gave noticeable image correction in

spite of adverse conditions. Future improvements to the P-WFS alone are mostly software related and should include a faster real time system, integrating P-WFS wavefront reconstruction and command matrices calculation in object-oriented mode and also WFS camera firmware upgrade to reduce jitter and readout noise. More efficient calibration schemes including zonal as well as modal control will allow a larger number of corrected modes. A second observing campaign will be planned when these software upgrades as well as fixes on the AO on-sky test bench are implemented.

REFERENCES

[1] Turbide, S. *et al*., "Development of a pyramidal wavefront sensor test-bench at INO," in [Adaptive Optics for Extremely Large Telescopes III], AO4ELT3 Conference Proceedings (2013).

[2] Martin, O. *et al*., "Pyramidal Wavefront Sensor Demonstrator at INO," Proc. of SPIE Vol. 9148, 91485X (2014).

[3] Brousseau, D. *et al*., "On-Sky AO Test Bench: Testing Future AO Technologies," in [Adaptive Optics for Extremely Large Telescopes IV], AO4ELT4 Conference Proceedings (these proceedings).

[4] Ragazzoni, R., J. Mod. Opt. **43**, 289, (1996).

[5] Esposito, S. *et al*., "Natural guide star adaptive optics system at LBT: FLAO commissioning and science operation status," Proc. SPIE 8447, 84470U (2010).